

Title	Prediction of potentially unstable electrical activity during embryonic development of rodent ventricular myocytes
Sub Title	
Author	大久保, 周子(Okubo, Chikako)
Publisher	慶應義塾大学湘南藤沢学会
Publication year	2012
Jtitle	生命と情報 No.19 (2012.) ,p.89- 98
JaLC DOI	
Abstract	Early embryonic rodent ventricular cells exhibit spontaneous action potential (AP), which disappears in later developmental stages. In this study, we used 2 mathematical models —the Kyoto and Luo-Rudy models— to overview the functional landscape of developmental changes in embryonic ventricular cells and predict potentially unstable APs. By switching the relative activities of 9 ionic components, of 512 representative combinations, the Kyoto model predicted 208 combinations to result in quiescent cells and 160 combinations to have regular spontaneous APs. The remaining 144 combinations were predicted to be potentially unstable, resulting from combinations of funny current (I _f), inward rectifier current (I _{k1}), sustained inward current (I _{st}), L-type Ca ²⁺ current (I _{caL}), and Na ⁺ current (I _{Na}). The Luo-Rudy model was used to verify the results. Based on these results, we suggest that sequential switches in the relative activities of I _{Na} , I _f , and I _{k1} enable ventricular cells to avoid unstable patterns.
Notes	慶應義塾大学湘南藤沢キャンパス先端生命科学研究会 2012年度学生論文集 卒業論文ダイジェスト
Genre	Technical Report
URL	https://koara.lib.keio.ac.jp/xoonips/modules/xoonips/detail.php?koara_id=KO92001004-00000019-0089

慶應義塾大学学術情報リポジトリ(KOARA)に掲載されているコンテンツの著作権は、それぞれの著作者、学会または出版社/発行者に帰属し、その権利は著作権法によって保護されています。引用にあたっては、著作権法を遵守してご利用ください。

The copyrights of content available on the KeiO Associated Repository of Academic resources (KOARA) belong to the respective authors, academic societies, or publishers/issuers, and these rights are protected by the Japanese Copyright Act. When quoting the content, please follow the Japanese copyright act.

Prediction of potentially unstable electrical activity during embryonic development of rodent ventricular myocytes

Department of Environment and Information Studies, Keio University

Chikako Okubo

ABSTRACT

Early embryonic rodent ventricular cells exhibit spontaneous action potential (AP), which disappears in later developmental stages. In this study, we used 2 mathematical models—the Kyoto and Luo-Rudy models—to overview the functional landscape of developmental changes in embryonic ventricular cells and predict potentially unstable APs. By switching the relative activities of 9 ionic components, of 512 representative combinations, the Kyoto model predicted 208 combinations to result in quiescent cells and 160 combinations to have regular spontaneous APs. The remaining 144 combinations were predicted to be potentially unstable, resulting from combinations of funny current (I_f), inward rectifier current (I_{K1}), sustained inward current (I_{st}), L-type Ca^{2+} current (I_{CaL}), and Na^+ current (I_{Na}). The Luo-Rudy model was used to verify the results. Based on these results, we suggest that sequential switches in the relative activities of I_{Na} , I_f , and I_{K1} enable ventricular cells to avoid unstable patterns.

Keywords: computer simulation, ion channels, ventricular cells, development, electrophysiology

1. Introduction

In rodents, spontaneous action potentials (APs) have been reported for the EE stage of developing rodent ventricular myocytes, eventually disappearing in passive contracting cells in the LE stage [2]. The electrophysiological properties of individual ion channels have been investigated in isolated ventricular myocytes at the representative 4 stages via patch clamp methods [3–5]. In addition to regular spontaneous APs, irregular and unstable APs have been reported in single mouse embryonic myocytes [6]. Although the existence of such irregular activities in single cells has been reported at the representative stages, potentially unstable activities must also be identified between the stages, along with the mechanisms underlying these activities, in order to elucidate the entire course of development of the heart.

Previously, we modeled developmental changes in the APs of cardiac ventricular myocytes [7] using the Kyoto model [8] and the Luo-Rudy model [9]. Measured APs at developmental stages were reproduced using common sets of these models by varying the relative activities of the ionic currents, pumps, exchangers, and sarcoplasmic reticulum (SR) Ca^{2+} kinetics. In addition, Jonsson *et al.* (2012) combined molecular biology and computer simulations to demonstrate that human embryonic stem cell-derived cardiomyocytes (hESC-CM) have an immature electrophysiological phenotype, based on insufficient function of inward rectifier K^+ current (I_{K1}) channels and a shift in the activation of sodium channels [10]. Thus, computer simulation is a powerful approach for confirming experimental data and providing insights into possible functional mechanisms involved in cardiac development.

2. Materials and Methods

Previously, we modeled developmental changes in the APs of cardiac ventricular myocytes using the Kyoto model and the Luo-Rudy model. Measured APs at developmental stages were reproduced using common sets of these models by varying the relative activities of the ionic currents, pumps, exchangers, and SR Ca^{2+} kinetics.

Briefly, quantitative changes in various ionic components were represented as the activities of the components in developmental stages relative to those in the adult stage. These relative activities were computed from current-voltage (I - V) curves or estimated based on qualitative observations as relative activities, and were then multiplied by the corresponding conductance (pA/mV) or conversion factors (pA/pF·mM) to demonstrate that developmental changes in the APs can be reproduced using common sets of mathematical equations. We adopted the same procedure in the present study and reconstructed EE and LE ventricular cell models using the updated Kyoto model. Table 1 lists the membrane currents that quantitatively change during embryonic development.

2.1 Switching the relative activities of the ionic components

We selected the following 9 components to be switched between the EE and LE stages: I_f , I_{st} , I_{K1} , Na^+ current (I_{Na}), L-type Ca^{2+} current (I_{CaL}), $\text{Na}^+/\text{Ca}^{2+}$ exchange current (I_{NaCa}), transient outward current (I_{to}), ATP-sensitive K^+ current (I_{KATP}), and a set of 4 electrical components of the SR. The

electrical components of the SR—which included the permeability of Ca^{2+} in the diadic space of Ca^{2+} release through the RyR channel in the SR (I_{RyR}), Ca^{2+} leak from the SR ($I_{\text{SR,leak}}$), the SR Ca^{2+} pump (I_{SRCA}), and Ca^{2+} transfer from the SR uptake site to the release site ($I_{\text{SR,transfer}}$)—were treated as a set of components in the SR because all 4 components are located in the SR and develop along with development of the SR. The other ionic components in the model were assumed to have constant current densities during embryonic development.

Table 1 Relative activities for ionic currents obtained from the literature

	EE	Reference	LE	Reference
I_{Na}	0.07		1.00	
I_{CaL}	0.46		0.78	
I_{K1}	0.11		1.00	
I_{KATP}	0.32		0.88	
I_{to}	0.01		0.27	
I_{NaCa}	4.95		1.74	
I_{SRCA}	0.03		0.21	
I_{RyR}	0.05		0.40	
$I_{\text{SR,transfer}}$	0.04	Estimated	0.30	Estimated
$I_{\text{SR,leak}}$	0.04	Estimated	0.30	Estimated
CICR	-3	Estimated	-60	Estimated

The relative activities were as reported previously [1]. In our previous study [1], we defined that the EE stage corresponds approximately 9.5-days post coitum (dpc) mouse and 11.5-dpc rat, and the LE stage corresponds to 1–5 days before birth.

2.2 Computer simulation procedures

We simulated 512 combinations of intact EE models for 600 s, switching the relative activities of the 9 components between EE and LE values. For those combinations that showed no spontaneous activity for 600 s, we applied external stimulation (-1500 pA) at 2 different frequencies (2.5 and 1.0 Hz) to determine whether the intact cells functioned as passive contracting cells. We classified the simulation results for the 512 combinations according to their electrical activities and identified potentially unstable patterns. We also predicted the specific order of switches in the relative activities that would avoid the potentially unstable patterns, assuming that each of the 9 components switches its activity from EE to LE, one by one.

We further verified our predictions by simulations with the Luo-Rudy model [10]. The relative activities of I_{Na} , I_f , I_{K1} , I_{CaL} , and SR-related components were switched between EE and LE values. Although the original Luo-Rudy model does not contain I_f , we implemented a mathematical model for I_f . The other components, I_{to} , I_{KATP} , I_{st} , and I_{NaCa} , were not considered in the simulations with the Luo-Rudy model. Switching the 5 components between EE and LE levels involved 32 combinations, which we simulated for 600 s, as well as additional 600-s simulations with external stimulation (-80 pA/pF at 2.5 Hz) for those combinations without spontaneous activities. Unlike the Kyoto model, the Luo-Rudy model does not include a consideration of cell capacitance; it was therefore not necessary to normalize

the activity at the developmental stages.

3. Results

Of the 512 combinations simulated using the Kyoto model, 208 combinations were predicted to result in quiescent cells with no spontaneous activity, and 192 of these combinations had quiescent membrane potentials (MPs) below -80 mV at 600 s. We observed spontaneous APs in the remaining 304 combinations, consisting of 160 regular spontaneous APs and 144 potentially unstable APs. Because the values of I_{KATP} , I_{to} , I_{NaCa} , and SR-related components did not significantly influence the simulation results, we focused on the remaining 5 pivotal currents, I_{Na} , I_f , I_{K1} , I_{st} , and I_{CaL} (Fig. 1).

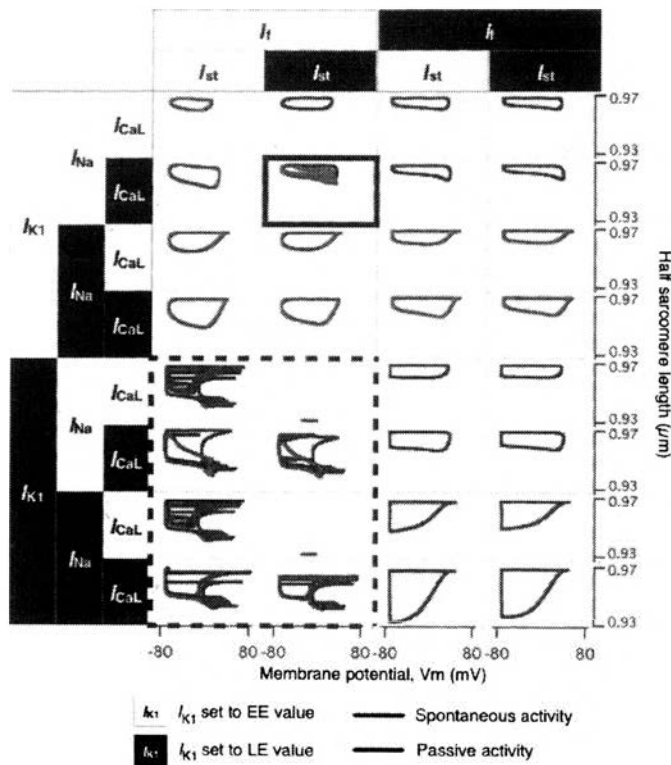


Figure 1 Simulated MP and hSL of 32 representative combination

The relative activities of I_{Na} , I_f , I_{K1} , I_{st} , and I_{CaL} were switched independently, yielding 32 combinations; those of the remaining 4 components were fixed to their EE values. MPs are represented on the horizontal axis (ranging from -88.25 to 85.5 mV) and half sarcomere lengths are on the vertical axis (ranging from 0.93 to 0.97 μm). Models with MP activities are presented as hysteresis loops, beginning at the upper left representing their maximum diastolic potential (MDP) and turning clockwise. Potentially unstable combinations are highlighted with solid and dashed boxes shown in detail in Figure 3.2 a and b. The horizontal and vertical axes in the dashed box range from -83.25 to 27.95 mV and from 0.81 to 0.94 μm , respectively. The hysteresis loops are illustrated based on profiles from 590 to 600 s for the intact simulations and 500 to 600 s for the models shown in the solid box.

Activities of I_f , I_{K1} , I_{st} , and I_{CaL} determined potentially unstable patterns. 128 combinations out of 512 were predicted to have 2 RMPs, at -35 mV and under -60 mV, when the relative activity of I_{K1} was set to the LE value and that of I_f was set to the EE value, regardless of the other three components (Fig. 1, dashed box and Fig. 2a). The MP was depolarized when the Ca^{2+} -activated background cation current (I_{LLCa}), which is activated when the intracellular Ca^{2+} concentration ($[\text{Ca}^{2+}]_i$) is high (Fig. 2a).

In 16 combinations, burst-like APs were observed when the relative activities of I_{CaL} and I_{st} were set to the LE values while those of I_{Na} , I_f , and I_{K1} were set to the EE values (Fig. 1, solid box). Figure 2b show the interval between the bursts was approximately 70 s at -50 mV. As the repetitive bursts were terminated, the Na^+/K^+ pump current (I_{NaK}) became dominant, and I_{NaK} gradually decreased during the quiescent state between the bursts. These combinations failed to produce normal APs in response to

application of external stimulus.

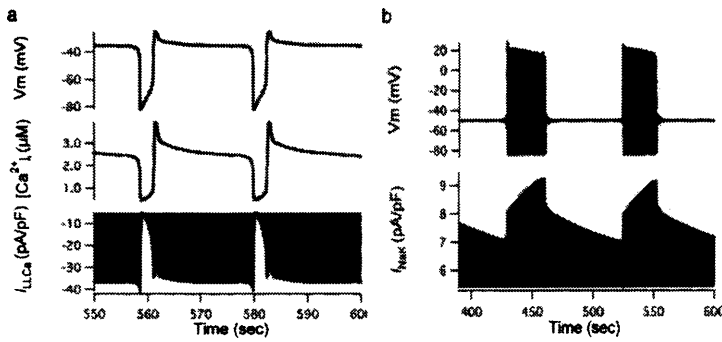


Figure 2 Simulated unstable combinations

(a) An unstable combination in which the relative activity of I_{K1} was set to the LE value and those of the other components were set to the EE values. (b) Burst-like activity was observed when the relative activities of I_{st} and I_{CaL} were set to the LE values and those of the other components were set to the EE values.

3.1 Application of external stimulus to quiescent models

The resting cell combinations were further simulated with external stimulus at a different frequency, and 56 combinations of the 208 failed to exhibit stronger contractions with external stimulus at 2.5 Hz than at 1.0 Hz. The amplitude of hSL at high frequency (2.5 Hz) was slightly smaller than that at low frequency (1.0 Hz) when the relative activities of I_f and I_{K1} were set to the LE values and those of the other components fixed to the EE values (Fig. 3a). On the other hand, when the relative activity of I_{Na} was switched to the LE value in addition to those of I_f and I_{K1} , the amplitude of hSL was twice as large with stimulus at 2.5 Hz than at 1.0 Hz.

The difference in hSL amplitudes resulted from larger Ca^{2+} influx via the reverse mode of I_{NaCa} and Ca^{2+} release from the SR via the RyR channel (Fig. 3c). The peak $[Ca^{2+}]_i$ was larger in models with the relative activity of I_{Na} switched to the LE value ($0.29 \mu M$) than in models with I_{Na} fixed to the EE value ($0.10 \mu M$) when the models were externally stimulated at 2.5 Hz. The difference resulted from larger Ca^{2+} influx via I_{NaCa} and Ca^{2+} release from the SR. In addition, we observed a subtle decrease in resting intercellular Na^+ concentrations ($[Na^+]_i$) from the LE (2.30 mM) to the adult (2.22 mM) models, and $[Na^+]_i$ was even higher when the relative activities of I_{Na} , I_f , and I_{K1} were switched to the LE from the EE model (2.33 mM). $[Na^+]_i$ was relatively low, however, when only the relative activities of I_f and I_{K1} were switched to the LE from the EE model (1.46 mM).

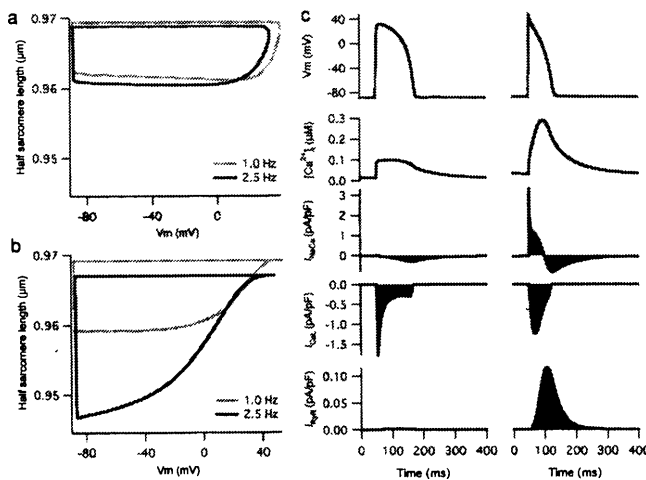


Figure 3 Tracings of MP, hSL, ionic currents, and $[Ca^{2+}]_i$ for the stimulated combinations

The relative activity of I_{Na} was set to the EE value (a) or LE value (b), while those of I_{K1} and I_f were set to the LE values and the other components were set to the EE values. External stimulus was applied at frequencies of 1.0 Hz (light lines) and 2.5 Hz (bold lines). (c) MP, $[Ca^{2+}]_i$, and accompanying ionic currents (I_{NaCa} , I_{CaL} , and I_{RyR}) of the models presented in (a) and (b); the relative activity of I_{Na} was set to the EE value (left) and the LE value (right) with external stimulus at 2.5 Hz

3.2 Simulated action potentials with the Luo-Rudy model

Eight of the combinations in the Luo-Rudy model failed to produce APs despite application of external stimulus (Fig. 4) when the relative activity of I_f was set to the LE values and those of all the other components were set at the EE values. In addition, these 8 combinations in Luo-Rudy model were among the combinations that defined unstable patterns in the Kyoto model with 2 RMPs. However, the 2 RMPs were not observed in the Luo-Rudy model.

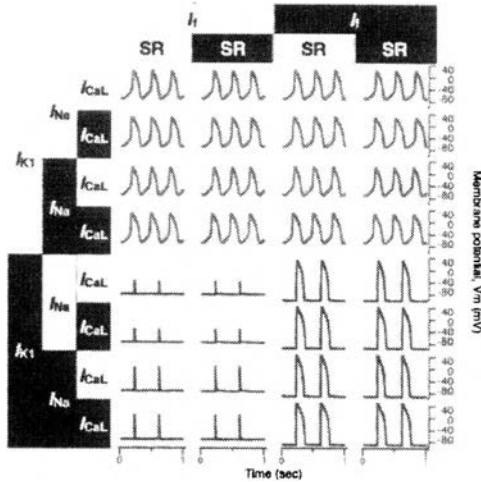


Figure 4 Simulated MPs for 32 combinations using the Luo-Rudy model

The relative activities of I_{Na} , I_{CaL} , I_f , I_{K1} , and SR-related components were switched independently between the EE and LE values. Spontaneous APs, represented as red traces, were observed when the relative activity of I_{K1} was set to the EE value. Spontaneous APs disappeared when the relative activity of I_{K1} was set to the LE value, and external stimulus was applied to produce an AP, represented as blue traces. All of the traces are illustrated based on the simulated results for 599 to 600 s.

3.3 Sequence of changes in I_{Na} , I_f , and I_{K1} to avoid predicted unstable patterns

Figure 5 shows changes in the APs and accompanying ionic currents as we sequentially switched I_{Na} , I_f , and I_{K1} from the EE model; spontaneous APs disappeared when I_{Na} , I_f , and I_{K1} were all switched to LE values, although AP was inducible by external stimulus. The maximum diastolic potential (MDP) gradually shifted in the negative direction and the overshoot potential became larger as I_{Na} increased, followed by disappearance of I_f (Table 2). The basic cycle length (BCL) of the model with I_{Na} switched to the LE value was shortest (0.34 ms) among the three spontaneous APs; the BCL was originally 0.51 ms in the EE model with disappearance of I_f . The peak amplitude of I_{CaL} decreased from -100 pA to -10 pA and that of I_{Na} increased from 0 pA to -5000 pA, and I_{Na} became responsible for rapid depolarization rather than I_{CaL} .

Table 2 Characteristics of representative spontaneous action potentials

Combinations	MDP (mV)	Overshoot potential (mV)	BCL (s)	DSD (s)
EE model	-81.40	2.14	0.51	0.30
I_{Na} set to LE	-82.48	37.16	0.34	0.13
I_{Na} and I_f set to LE	-84.73	53.66	0.78	0.52

Values of MDP, Overshoot potential, BCL, and diastolic slow depolarization (DSD) of a spontaneous AP were recorded during the last spontaneous AP of the 600-s simulation.

4. Discussion

We predicted unstable membrane excitation patterns from among computer simulations of 512 combinations and identified I_{Na} , I_f , I_{K1} , I_{CaL} , and I_{st} as components potentially responsible for the predicted unstable patterns (Fig. 1). To avoid unstable patterns with 2 RMPs (Fig. 2a), burst-like MPs (Fig. 2b), and failure to stronger shortening force at 2.5 Hz than at 1.0 Hz (Fig. 3a,b), we suggest that I_{CaL} and I_{st} should not be switched before an increase in I_{Na} , and demonstrated that sequential switching of I_{Na} , I_f , and I_{K1} could avoid unstable patterns (Fig. 4).

4.1 Required order of I_f and I_{K1} switching to avoid unstable patterns

We observed abnormally high $[Ca^{2+}]_i$ values in combinations with 2 RMPs, -85 mV and -35 mV (Fig. 2a), when I_{K1} increased before disappearance of I_f . The simulated $[Ca^{2+}]_i$ were approximately 4.0 μ M, leading to activation of I_{LCCa} , a current whose open probability increases at high $[Ca^{2+}]_i$ and contributes to transient inward current [26]. The activated I_{LCCa} contributed to depolarization of the membrane to -35 mV and deactivation of I_{LCCa} ; subsequent activation of I_f resulted in repolarization of the membrane to -80 mV. Abnormally high $[Ca^{2+}]_i$ was observed when I_{K1} increased approximately 10-fold (from 0.11 to 1.0) before disappearance of I_f (from 1.0 to 0.0) (Fig. 3). Because of the abnormally high $[Ca^{2+}]_i$, we designated these combinations as unstable patterns, and suggest that I_f should disappear before I_{K1} increases to avoid unstable patterns with 2 RMPs. The above hypothesis is consistent with previous experimental reports on developing cardiomyocytes and hESC-CM. I_f is known to be a pacemaker current and plays an important role in spontaneous firing of APs in 9.5-dpc mice, but decreases by 80% by 18 dpc. In contrast, the current density of I_{K1} is very small in 12-dpc rats, and increases nearly 10-fold by the end of embryonic development, contributing to a negative shift in RMP. In addition, an immature electrophysiological phenotype for hESC-CM has been reported with insufficiently functional I_{K1} channels.

Moreover, 8 of the 32 combinations in the Luo-Rudy model failed to produce APs despite application of external stimulus when the relative activity of I_f was set to the LE values and those of all the other components were set at the EE values (Fig. 4). These 8 combinations in Luo-Rudy model were among the combinations that defined unstable patterns in the Kyoto model with 2 RMPs. However, the 2 RMPs were not observed in the Luo-Rudy model.

4.2 An increase in I_{CaL} and disappearance of I_{st} are responsible for burst-like MP

An unstable pattern exhibiting burst-like MPs (Fig. 2b) has been reported in the pulmonary vein of rodents. In our simulations, burst-like MPs were observed when the relative activities of I_{st} and I_{CaL} were set to the LE values and those of I_{Na} , I_f , and I_{K1} were set to the EE values. I_{st} has been reported as ionic currents of Ca^{2+} and K^+ and has been observed only in SAN cells, but there is no evidence for I_{st} in embryonic rodents. We also have no evidence for I_{st} or burst-like activities in developing ventricular cells. However, we suggest that combinations that showed burst-like activities need to be avoided during embryonic development since such activities in the pulmonary vein are known to cause atrial fibrillation.

Burst-like APs are attributed to a balance between negative and positive currents; as such, the

duration of the repetitive bursts changes as the activities of other components are switched, including I_{Kr} , I_{KATP} , I_{to} , and SR components (data not shown). We identified I_{NaK} as a principal component in initiating the bursts, because the outward Na^+ current and inward K^+ current via I_{NaK} became dominant over the opposite currents and I_{NaK} gradually decreased during the quiescent state between bursts (Fig. 2b).

4.3 An early increase in I_{Na} appears required for embryonic developmental

We suggest that I_{Na} should be switched to the LE level before I_f and I_{K1} to reflect changes in $[Na^+]_i$ and $[Ca^{2+}]_i$ during embryonic development reported in the literature . $[Na^+]_i$ was higher in combinations in which the relative activities of I_{Na} , I_f , and I_{K1} were set to the LE values (2.33 mM) and in the LE model (2.30 mM) vs. the adult model (2.22 mM) in their resting states (Table 3.1). These results are consistent with a report that $[Na^+]_i$ in EE ventricles was higher than in more developed embryos, while intracellular K^+ concentration ($[K^+]_i$) remained constant throughout embryonic development in the chick . In addition, dynamic changes in Na^+ channel expression are evident within the first 5 days of embryonic development in both mice and chicks . In contrast, in combinations in which the relative activities of I_f and I_{K1} were set to the LE values, $[Na^+]_i$ was lower (1.46 mM) than in the others.

An increase in I_{Na} density is responsible for the large amplitude of $[Ca^{2+}]_i$ and strong contractions with high-frequency external stimulus. Although the amplitude of hSL was larger at 2.5 Hz than at 1.0 Hz regardless of I_{Na} density, differences between the amplitudes of hSL at 2.5 Hz and 1.0 Hz were larger when I_{Na} was switched to LE values (Fig. 3.3 b) than at EE values (Fig. 3.3 a); $[Ca^{2+}]_i$ was more than twice as large at 2.5 Hz (0.291 μ M) than at 1.0 Hz (0.116 μ M) when the I_{Na} density increased (Table 3.1). This change in $[Ca^{2+}]_i$ is consistent with a report that $[Ca^{2+}]_i$ in adult myocytes was 3 times that in fetal myocytes .

Switching I_{Na} from EE to LE levels changed the source of the Ca^{2+} influx necessary for contraction. The Ca^{2+} influx via the reverse mode of I_{NaCa} was greater when I_{Na} was switched to the LE level; the large Ca^{2+} influx through I_{CaL} and then I_{NaCa} triggered Ca^{2+} release from the SR via the RyR channel, which consequently resulted in a large $[Ca^{2+}]_i$ transient (Fig. 3c). An increase in the relative activities of I_{CaL} and SR-related components and a decrease in I_{NaCa} resulted in larger amplitudes of hSL and $[Ca^{2+}]_i$ transients, and an increase in I_{Na} further enhanced the effect of switches in I_{CaL} , I_{NaCa} , and SR-related components on the amplitudes of hSL. Based on these results, we suggest that I_{Na} should be increased early to increase the Ca^{2+} influx through I_{CaL} and the Ca^{2+} release through the RyR channel on the SR.

4.4 I_{Na} , I_f , and I_{K1} are sequentially switched from EE to LE levels

The simulation results imply that I_{Na} should increase before disappearance of I_f , followed by an increase in I_{K1} . Following the sequence with representative models (Fig. 5), we observe that I_{Na} took over the role of I_{CaL} , which was originally the current responsible for depolarization of the membrane in

the EE model. This change in the dependence of depolarization from the Ca^{2+} current to the Na^+ current is consistent with experimental observations in rodent ventricular myocytes in which MDP shifted in a negative direction, also consistent with our simulation (Table 2). On the other hand, the BCL shortened when I_{Na} increased and lengthened when I_f disappeared (Fig. 5). EE hearts have a large range of heart rates, 61–219 min^{-1} in 11.5-dpc rats, and the beating rhythm of EE ventricular cells is generally slow and irregular. In addition, Yasui *et al.* (2001) reported that the BCL was irregular in 18.5-dpc mouse ventricular cells with spontaneous APs. Although all of the representative models shown in Figure 5 are within the range of the BCLs reported in vitro, our model was unable to reproduce the irregular spontaneous APs observed by Yasui *et al.* (2001) [6].

Of the 9 currents, unstable patterns were observed for specific combinations of switches in I_{Na} , I_{CaL} , I_f , I_{st} , and I_{K1} . In addition, I_{NaCa} and SR-related components were involved in enhancing cell contraction. The remaining 2 currents, I_{KATP} and I_{to} , were not responsible for unstable electrical activities or contraction in this study. Our hypothesis that an increase in I_{Na} density and disappearance of I_f should be observed in the early stage of embryonic development is supported by experimental observations that the activities of I_{Na} and I_f change more than those of other components, including I_{CaL} , I_{K1} , I_{NaCa} , and SR-related components. We demonstrate here that switching all of the components in the mathematical model enabled us to simulate all possible combinations, predict potentially unstable patterns, and identify indispensable component switches for avoiding the predicted unstable patterns. Our simulation procedure, together with experimental observations in the literature, will likely be useful in identifying sequential regulation of gene or protein expressions during development that are difficult to determine through experimental data alone.

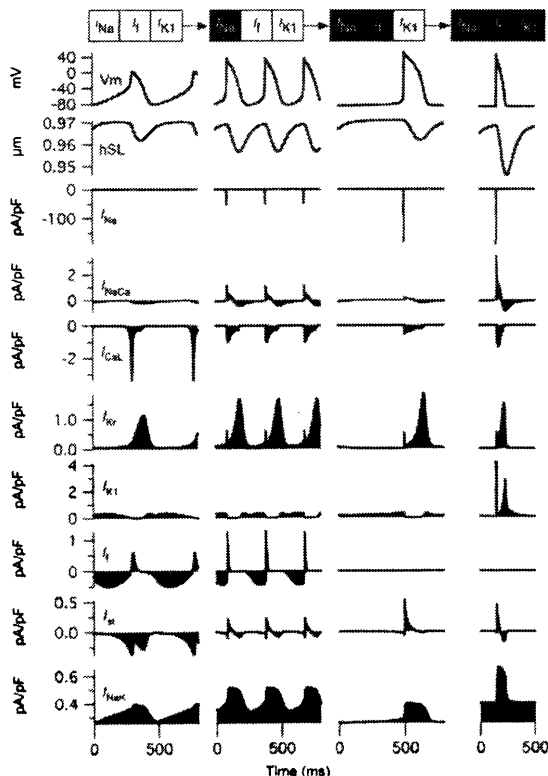


Figure 5 Simulated tracings of APs, hSL, and accompanying ionic currents

The relative activities of I_{Na} , I_f , and I_{K1} were sequentially switched to the LE values from the EE model. External stimulus (-1500 pA/pF) was applied to the model in which the relative activities of I_{Na} , I_f , and I_{K1} were all set to the LE values.

Conclusions

In the Kyoto and Luo-Rudy models, our simulation results suggested that I_f should disappear before the 10-fold increase in I_{K1} to avoid potentially unstable patterns. Of the 9 components switched between EE and LE levels in the Kyoto model, combinations of switches in I_{Na} , I_{CaL} , I_f , I_{st} , and I_{K1} densities were responsible for potentially unstable patterns.

References

1. Itoh H, Naito Y, Tomita M (2007) Simulation of developmental changes in action potentials with ventricular cell models. *Syst Synth Biol* 1: 11-23.
2. Matsuoka S, Sarai N, Kuratomi S, Ono K, Noma A (2003) Role of individual ionic current systems in ventricular cells hypothesized by a model study. *Jpn J Physiol* 53: 105-123.
3. Faber GM, Rudy Y (2000) Action potential and contractility changes in $[Na^+]_i$ overloaded cardiac myocytes: a simulation study. *Biophys J* 78: 2392-2404.
4. Kuzumoto M, Takeuchi A, Nakai H, Oka C, Noma A, et al. (2008) Simulation analysis of intracellular Na^+ and Cl^- homeostasis during beta 1-adrenergic stimulation of cardiac myocyte. *Prog Biophys Mol Biol* 96: 171-186.
5. Kurata Y, Matsuda H, Hisatome I, Shibamoto T (2007) Effects of pacemaker currents on creation and modulation of human ventricular pacemaker: theoretical study with application to biological pacemaker engineering. *Am J Physiol Heart Circ Physiol* 292: H701-718.
6. Yasui K, Liu W, Opthof T, Kada K, Lee JK, et al. (2001) $I(f)$ current and spontaneous activity in mouse embryonic ventricular myocytes. *Circ Res* 88: 536-542.
7. Masuda H, Sperelakis N (1993) Inwardly rectifying potassium current in rat fetal and neonatal ventricular cardiomyocytes. *Am J Physiol* 265: H1107-1111.
8. Jonsson MK, Vos MA, Mirams GR, Duker G, Sartipy P, et al. (2012) Application of human stem cell-derived cardiomyocytes in safety pharmacology requires caution beyond hERG. *J Mol Cell Cardiol*.
9. Namekata I, Tsuneoka Y, Akiba A, Nakamura H, Shimada H, et al. (2010) Intracellular calcium and membrane potential oscillations in the guinea pig and rat pulmonary vein myocardium. *Bioimages* 18: 11-22.
10. Guo J, Ono K, Noma A (1995) A sustained inward current activated at the diastolic potential range in rabbit sino-atrial node cells. *J Physiol* 483 (Pt 1): 1-13.
11. de Bakker JM, Ho SY, Hocini M (2002) Basic and clinical electrophysiology of pulmonary vein ectopy. *Cardiovasc Res* 54: 287-294.
12. Haissaguerre M, Jais P, Shah DC, Takahashi A, Hocini M, et al. (1998) Spontaneous initiation of atrial fibrillation by ectopic beats originating in the pulmonary veins. *N Engl J Med* 339: 659-666.
13. Klein RL (1963) High Na Content of Early Embryonic Chick Heart. *American Journal of Physiology* 205: 370-&.
14. Seki S, Tribulova N, Manoach M, Mochizuki S (2003) Modulation of intracellular Ca^{2+} concentration by tedisamil, a class III antiarrhythmic agent, in isolated heart preparation. *Life Sci* 73: 1805-1811.
15. Davies MP, An RH, Doevendans P, Kubalak S, Chien KR, et al. (1996) Developmental changes in ionic channel activity in the embryonic murine heart. *Circ Res* 78: 15-25.
16. Fujii S, Ayer RK, Jr., DeHaan RL (1988) Development of the fast sodium current in early embryonic chick heart cells. *J Membr Biol* 101: 209-223.
17. DeHaan RL, Fujii S, Satin J (1990) Cell interactions in cardiac development. *Development Growth & Differentiation* 32: 233-241.
18. Couch JR, West TC, Hoff HE (1969) Development of the action potential of the prenatal rat heart. *Circ Res* 24: 19-31.
19. Nagashima M, Tohse N, Kimura K, Yamada Y, Fujii N, et al. (2001) Alternation of inwardly rectifying background K^+ channel during development of rat fetal cardiomyocytes. *J Mol Cell Cardiol* 33: 533-543.
20. Kato Y, Masumiya H, Agata N, Tanaka H, Shigenobu K (1996) Developmental changes in action potential and membrane currents in fetal, neonatal and adult guinea-pig ventricular myocytes. *J Mol Cell Cardiol* 28: 1515-1522.
21. Artman M (1992) Sarcolemmal Na^+ - Ca^{2+} exchange activity and exchanger immunoreactivity in developing rabbit hearts. *Am J Physiol* 263: H1506-1513.
22. Liu W, Yasui K, Opthof T, Ishiki R, Lee JK, et al. (2002) Developmental changes of Ca^{2+} handling in mouse ventricular cells from early embryo to adulthood. *Life Sci* 71: 1279-1292.
23. Kilborn MJ, Fedida D (1990) A study of the developmental changes in outward currents of rat ventricular myocytes. *J Physiol* 430: 37-60.
24. Xie LH, Takano M, Noma A (1997) Development of inwardly rectifying K^+ channel family in rat ventricular myocytes. *Am J Physiol* 272: H1741-1750.